Biosensors and Bioelectronics, Volume 23, Issue 3, 31 October 2007, Pages 377-383

# The study of genomic DNA adsorption and subsequent interactions using Total Internal Reflection Ellipsometry

**Alexei Nabok[+], Anna Tsargorodskaya[+], Frank Davis[++], Séamus P.J. Higson[++] ***

[+] *Sheffield Hallam University, Materials and Engineering Research Institute, Sheffield, S1 1WB, U.K.*

[++] *Cranfield Health, Cranfield University, Silsoe, MK45 4DT, U.K.*

* Correspondence should be addressed to s.p.j.higson@cranfield.ac.uk.

The adsorption of genomic DNA and subsequent interactions between adsorbed and solvated DNA was studied using a novel sensitive optical method of total internal reflection ellipsometry (TIRE), which combines spectroscopic ellipsometry with surface plasmon resonance (SPR). Single strands of DNA of two species of fish (herring and salmon) were electrostatically adsorbed on top of polyethylenimine films deposited upon gold coated glass slides. The ellipsometric spectra were recorded and data fitting utilized to extract optical parameters (thickness and refractive index) of adsorbed DNA layers. The further adsorption of single stranded DNA from an identical source, i.e. herring ss-DNA on herring ss-DNA or salmon ss-DNA on salmon ss-DNA, on the surface was observed to give rise to substantial film thickness increases at the surface of about 20-21 nm. Conversely adsorption of DNA from alternate species, i.e. salmon ss-DNA on herring ss-DNA or herring ss-DNA on salmon ss-DNA, yielded much smaller changes in thickness of 3-5 nm. AFM studies of the surface roughness of adsorbed layers were in line with the TIRE data.

## 1. Introduction

Despite great recent progress in DNA analytical technology, that has become routine in a number of different fields, such as medicine, agriculture, food industry and forensic science, there is still a great demand that needs to be met for simple portable analytical tools for DNA characterization. Biosensing approaches for DNA analysis could offer a cost-effective alternative to expensive contemporary methods requiring the use of enzyme, fluorescent or radioisotope labels (Downs 1991). DNA biosensors are based on the concept of sequence-specific hybridization between nucleic acids in solution - and those immobilized on solid substrates (Ausubel *et al* 1993). For example, a number of DNA sensors exploiting immobilization of nucleic acids on conjugated polymers and different transducing techniques were reported (Korri-Youssufi *et al* 1997, Kumbupu-Kalemba and Leclerc 2000, Leclerc 1999, McQuade *et al* 2000).

The method of electrostatic layer-by-layer adsorption of DNA, which was first reported in the early 1990's (Lvov *et al* 1993, Sukhorukov *et al* 1996) has later become widely used in DNA sensors for immobilization of oligonucleotides (Xi *et al* 2000, Bjork *et al* 2005, Travas-Sejdic *et al* 2005) and whole DNA molecules (Cardenas *et al* 2003, Sato *et al* 2005). The concept of using a single strand DNA immobilized on solid support for further hybridization with its counterpart in the solution and the subsequent formation of DNA double helices on the surface has been exploited previously (Nicollini *et al* 1997, Mascini *et al* 2001, Lemeshko *et al* 2001), although the formation of the ideal DNA double helix is not obvious because of a limited mobility of the adsorbed single strand DNA.

Most of the work reported earlier has utilized short DNA fragments, usually containing <50 bases and of perfectly matched or a few base pair mismatched sequences, although cDNA arrays often use DNA of similar lengths for detection. Our work however has tended towards the use of genomic DNA rather than specific sequences since that is the form in which DNA naturally occurs. Genomic DNA can be easily denatured to form single-stranded DNA by heating, however upon cooling, hybridisation back to the double-stranded form is a complex procedure. This is probably because genomic DNA contains a wide variety of individual chains with different lengths and sequences and the statistical probability of two complementary chains meeting and hybridizing is very low. Even when DNA from a single species is allowed to reassociate, measurements have showed that the nucleotide pairing is imprecise (Britten and Kohne 1968). The extent of reassociation between DNA of different species has also been studied and shown to be a measure of the relationship between the species (Martin and Hoyer 1966).

This led us to attempt to determine whether adsorbed genomic DNA would display increased interactions with genomic DNA from the same species compared to DNA from a different species. Although it is very unlikely that we would see complete hybridization due to the reasons given above, it was thought that there may still be more interaction between two samples of single stranded DNA of similar composition than two samples from different species (Martin and Hoyer 1966). This could potentially lead to a simple DNA sensor capable of quickly and inexpensively determining the identity of components in, for example, foodstuffs and/or fabrics made from natural materials.

In a previous publication by ourselves (Davis *et al* 2005), a layer of single stranded DNA was electrostatically adsorbed on different surfaces for use as a recognition template in electrochemical DNA sensors. An optical method of conventional external reflection ellipsometry was also deployed in this work as a second and complementary technique to monitor DNA interactions. The above electrochemical and ellipsometry measurements have resulted in clear differentiation of DNA in two species of fish: herring and salmon (Davis *et al* 2005). Response times were of the order of 10-60 minutes, depending on concentration, for the electrochemical measurements. The limit of detection was 0.01 mg/ml, which is much less sensitive than reported for many other authors. However they were often utilizing relatively short DNA strands of a single sequence rather than genomic DNA. When we utilized single gene DNA in our work (Davis *et al* 2007), sensitivity was greatly increased, capable of detection of levels of DNA down to 1fg/ml. This compares favourably with many other techniques although lower levels of DNA have been detected by utilising electroactive species which bind strongly to double stranded DNA, enabling detection of $10^{-19}$ moles of oligonucleotide (Park and Hahn 2004). An enzyme-catalysed metallization process may also be used to electrochemically detect hybridisation of as little as $10^{-20}$ moles of an oligonucleotide (Hwang *et al* 2005).

In the present work, a detailed study of DNA electrostatic immobilization and further DNA interactions was carried out using an advanced optical technique of total internal reflection ellipsometry (TIRE), as well as via direct observation of absorbed DNA layers with atomic force microscopy (AFM). The sensitivity of TIRE is approximately ten times greater than that of conventional ERE (Nabok *et al* 2007, Nabok and Tsargorodskaya 2007), potentially making small changes in film thickness and morphology much easier to detect. Our previous papers (Davis *et al* 2005, 2007) concentrated mainly on the electrochemical responses and the sensitivity and specificity of the DNA recognition. The work presented in this paper is intended more as a study of the nature of the adsorbed layers and the kinetics of binding rather than development of a detection method, in an attempt to determine the behaviour of the DNA strands and the morphology of the films formed. To our knowledge this is the first time that

this technique has been applied to the study of DNA adsorption at surfaces, allowing details of the adsorption kinetics and film morphology to be determined.

## 2. Experimental.

### *2.1 Total Internal Reflection Ellipsometry.*

The method of Total Internal Reflection Ellipsometry (TIRE) (Posinski *et al* 2004, Arwin *et al* 2004) was exploited in this work to study the adsorption and hybridization of DNA molecules. This method combines the spectroscopic ellipsometry platform with the Kretchmann SPR geometry of coupling the beam through the prism to the thin film of metal (gold). The experimental set-up is described in detail within the supplementary information. The details of ellipsometry data fitting are given in the supplementary information.

All TIRE measurements were performed on samples immersed into the same phosphate buffer solution (pH 7). In addition to that, kinetic TIRE measurements were carried out by recording $\Psi(\lambda)$ and $\Delta(\lambda)$ spectra after a certain time interval typically of 20-30 seconds in the course of DNA adsorption (where $\Psi$ is the amplitude (A) ratio $\tan(\Psi) = A_p / A_s$ and $\Delta$ the phase shift $\Delta = \varphi_p - \varphi_s$ between *p*- and *s*- components of polarized light of wavelength $\lambda$). In these measurements, fitting was not performed because of possible interference due to changes of the refractive index of DNA solutions during the course of the experiment. Fitting was only performed before and after kinetic experiments were complete and whilst the cell is filled with phosphate buffer only. Kinetic curves were obtained by selecting $\Psi$ or/and $\Delta$ data points at a certain wavelength ($\lambda$) from a massive $\Psi$, $\Delta$ ($\lambda$, t) file and plotting respective time dependencies $\Psi(t)$, $\Delta(t)$. The shape (raising or decaying) of $\Psi(t)$, $\Delta(t)$ curves depends on the wavelength selection on either the decreasing or rising part of $\Psi(\lambda)$, $\Delta(\lambda)$ spectra, respectively.

### *2.2 AFM Measurements.*

AFM tapping mode images of adsorbed DNA layers were obtained using a Nanoscope IIIa instrument using silicon nitride tips of less than 10 nm in radius. The films for AFM study were deposited onto clean 10x10 mm pieces of silicon wafers. Typical scan rates used were about 1Hz and the oscillation frequency was around 400 kHz. Roughness analysis of the obtained images was performed using the integrated image processing software.

*2.3 DNA and chemicals.*

The preparation of the DNA solutions is described in the supplementary information. Our previous work (Davis *et al* 2005) showed that binding of DNA to polyethylenimine (PEI) layers and subsequent interactions could be easily measured when 0.2 mg/ml solutions in phosphate buffer (pH 7) were utilised, therefore solutions of this strength were used in this study. Single strand DNA (ss-DNA) was prepared by denaturizing of DNA double helix (or strand) (ds-DNA) by heating DNA solutions up to $95^0$C and its subsequent sharp cooling in ice (Davis *et al* 2005). The solution of ss-DNA was used as soon as possible to minimize any potential interactions or crosslinking in solution. RNA molecules (from Sigma Aldrich) having original single strand structure were used for comparison. RNA was chosen because although it has a single stranded structure, it can also exist in a helical structure similar to ds-DNA. Polyethyleneimine from Sigma Aldrich (mw=50000) was used in this work for electrostatic adsorption of DNA (in both single- and double- stranded forms) and RNA molecules onto solid substrates. At the pHs used the charge density of PEI corresponds to 20% of the amine groups being protonated (Suh *et al* 1994). Previous work (Davis *et al* 2005) indicates that the nature of the cationic polymer only has small effects on film behaviour. This is thought to be due to single stranded DNA having a lower charge density than any of the polycations we utilized, meaning that the cationic groups were in excess for all the polymers used. This meant that the limiting factors for DNA adsorption and the structures and the further behaviour of the DNA layers were not overly dependent on the nature of the anchoring layer.

The molecular weights of the DNA samples were determined by gel electrophoresis (details in supplementary information). The salmon DNA consisted mainly of material with a molecular size of 2000bp whereas the herring DNA had a more diverse spread of weight, between 300-1000bp.

*2.4. Sample preparation.*

The preparation of gold and silicon substrates and their treatment with PEI is described in the supplementary information. Previous workers have shown that amines will complex to gold surfaces (Leff *et al* 1996) through a charge-neutral weak covalent bond and a polyamine should therefore adhere to a gold surface extremely well. Freshly etched silicon surfaces bear a slight negative charge and thus electrostatic binding between Si and PEI will occur.

Layers of either ss-DNA, or ds-DNA, or RNA were electrostatically bound to the solid surface by either dipping the substrate into the solution as appropriate or by injecting the required solutions into the cell. In both cases the exposure time was 5 minutes. The samples were then rinsed with Millipore water either in a beaker or by purging the cell with at least three times the cell volume of water.

To study the interactions between adsorbed and solvated DNA with the TIRE method, solution of ss-DNA was injected into the cell and left for 3 hours. During this time, kinetic TIRE measurements were taken. After 3 hours only minimal further changes in the TIRE results could be observed. The excess of DNA was washed away by pumping Millipore water through the cell. TIRE spectra measurements were then repeated with the cell filled with phosphate buffer solution. The samples for AFM study were prepared by immersing the sample into the solution of single stranded DNA for 3 hours followed by thorough rinsing with Millipore water and drying at room temperature.

## 3. Results and discussion.

### *3.1 TIRE spectra.*

Typical TIRE spectra of Cr/Au films used in this work are shown in Fig. 1b. The spectrum of $\Psi(\lambda)$, representing the amplitude ratio of $A_p/A_s$, very much resembles a conventional SPR curve. In contrast, the spectrum of $\Delta(\lambda)$, which is related to the phase shift between p- and s- components of polarized light, experiences a sharp drop from $270^0$ down to $-90^0$ near the plasmon resonance. According to Arwin's modelling (Arwin *et al* 2004), the position of this drop on $\Delta(\lambda)$ spectra is about 10 times more sensitive to adsorption than $\Psi(\lambda)$ spectra and conventional SPR curves.

A typical TIRE spectra of DNA adsorption is shown in Fig. 2. As can be seen, adsorption of a very thin monolayer of PEI causes a tiny shift of the TIRE $\Delta(\lambda)$ spectra. Adsorption of a layer of either herring ss-DNA or salmon ss-DNA causes an additional shift (still small) of the $\Delta(\lambda)$ spectrum. Adsorption of a second layer of complementary ss-DNA, i.e. salmon ss-DNA on top of salmon ss-DNA (Fig. 2a) or herring ss-DNA on top of herring ss-DNA causes a large spectral shift of about 80-100 nm. At the same time, the adsorption of non-complementary ss-DNA, i.e. herring ss-DNA on top of salmon ss-DNA (Fig. 2b) or salmon ss-DNA on top of herring ss-DNA yields much smaller spectral shift of 40-60 nm.

Fitting of the experimental results was performed with WVASE® software using a four layers model, which is shown in Table 1 and described in more detail the supplementary information and in previous work (Nabok *et al* 2007, Nabok and Tsargorodskaya 2007).

Changes in the thickness of adsorbed layers (Layer 1) obtained by TIRE data fitting are shown in Table 2. The data for adsorption of ds-DNA of both herring and salmon as well as of RNA are also shown in Table 2 for comparison.

For herring DNA, the thickness of the adsorbed single strand DNA was found to be of 4.22 ± 1.72 nm, which is substantially less than the value of 12.96 ± 3.14 nm for adsorbed RNA molecules also representing a single polynucleotide chain. Such difference is not surprising considering RNA has a complex secondary structure with hairpin loops and helical fragments (Littauer 2000). The thickness of the adsorbed layer is somewhat higher than expected, indicating that we do not have a simple compact monolayer at the surface. It should be remembered however that our measurements take place with the film submerged in buffer, meaning that it will be fully hydrated. Other workers [Legay *et al* 2005] have shown that the thicknesses of DNA layers on a gold surface are much greater in a hydrated state than in a dry state. Longer DNA chains have been shown to have a quite flexible structure (Steel *et al* 2000) and there is also the possibility of looping of the DNA chains from the surface which would also have the effect of increasing the thickness of the adsorbed layer. When undenatured herring ds-DNA was utilised, the film thickness was much greater (9.75 ± 1.97 nm). This cannot be a simple monolayer of double-stranded DNA lying flat on the surface since this would only have a thickness of about 2 nm. Again however the layers are fully hydrated and there is also potential for supercoiling to occur, as observed by other workers on silicon surfaces (Rippe *et al* 1997).

Adsorption of a second layer of herring ss-DNA causes substantial increase in the layer thickness of 21.81 ± 1.09 nm. We believe we first have a hydrated layer of DNA electrostatically adsorbed onto the substrate. Interaction between complementary short sequences of bases on adsorbed and solvated DNA cause adsorption of a second layer of DNA, although it is certain that hybridization to a double helix will not occur. Since this interaction will only occur along a relatively short part of the DNA chain, their will be extensive looping out into the solution of the rest of the chain. These unbound chains could then further interact with each other or with other strands in solution. The final structure is that of a loosely bound, crosslinked multilayer.

Figure S2 (supplementary information) illustrates schematically main stages of adsorption, (a) electrostatic adsorption ss-DNA onto the PEI layer, (b) adsorption of complementary ss-DNA on top with parts of the strands pendant to the surface, (c) adsorption of further ss-DNA accompanied with crosslinking and tangling.

The adsorption of non-complementary ss-DNA (salmon) on top of adsorbed layer of herring ss-DNA has resulted in much smaller changes in the thickness (4.36 ± 0.36 nm) corresponding to a much

lower level of adsorption. There will always be some degree of interaction between long DNA strands because there will always be small sequences of a few bases that will match and cause some interaction, however, as this work shows, genomic DNA strands from the same source display a higher degree of interaction, leading to formation of thicker films.

A similar situation is observed for salmon DNA. The thickness of the electrostatically adsorbed ss-DNA-salmon layer was found to be of 4.08 ± 1.56. Adsorption of a second layer of salmon ss-DNA causes substantial increase in the layer thickness of 20.47 ± 0.53 nm which is very similar to that observed for herring DNA. Again, the thickness of salmon DNA adsorbed on the surface is larger than the thickness of adsorbed ds-DNA-salmon (8.52 ± 2.37). The adsorption of non-complementary ss-DNA (herring) on top of adsorbed layer of salmon ss-DNA has resulted in much smaller changes in the thickness (3.02 ± 1.15).

Surprisingly large thickness changes of 20-21 nm, which were observed after adsorption of complementary ss-DNA, can be explained by initial interaction to form a loosely bound second layer with extensive looping out of unbound chains. Further interaction could then stabilise the formation of a crosslinked multilayer structure. Super-coiling of DNA, which was reported recently to occur on a silicon surface could also have an effect (Rippe *et al* 1997).

The process of DNA hybridization accomplished by coiling up of two complementary single strands requires complete three-dimensional freedom for both counterparts and near-perfect matching of the bases. This is highly unlikely within our system where genomic DNA has been utilised and strands are immobilized on a surface. Interaction of adsorbed fragments of ss-DNA with short sequence matching fragments of complementary ss-DNA in solution is possible, however, and would give a structure with unbound chains looping into solution which with further interactions could lead to super-coiling, tangling and knotting of the resulting DNA structure (Delmont and Mann 2003). The resulted thickness of DNA layer is therefore much larger than anticipated. What is of interest is that this process is much less efficient when the adsorbed and solvated DNA come from different sources. Even though re-hybridisation to form the double helix is probably impossible, there is still a degree of selectivity which could be enough for the development of simple, species-selective DNA sensors.

The obtained thickness values of 8-9 nm for electrostatically adsorbed layers of DNA are larger than the value of 4.4±1.2 nm reported earlier for sturgeon DNA/PEI layers (Sukhorukov *et al* 1996). This is most probably due to the fact that the measurements in the literature were performed on dried films, whereas our samples are immersed and therefore full hydrated, which other workers have shown

to have a large effect on film thickness (Legay *et al* 2005). Other factors could be due to the difference in sample preparations and adsorption conditions.

*3.2. Kinetics study.*

Typical time dependencies of changes in the value of Δ at a certain wavelength near the resonance are shown in Fig. 3 for adsorption of both single and double stranded DNA of both species of fish. All curves presented are descending due to the choice of the wavelength on the rising section (on the left from the resonance) of the Δ(λ) spectrum, as indicated by the cross in Fig. 1b. Similar kinetic curves could be obtained from Ψ(λ) spectra. All kinetic curves follow a Langmuir type of adsorption. The results obtained are in line with the Δ(λ) spectra in Fig. 2 and their fitting in Table 1. For herring DNA (see Fig. 3a), the value of Δ at saturation increases in the following order: adsorption of herring ss-DNA on PEI layer, adsorption of non-complementary (salmon) ss-DNA on herring ss-DNA, adsorption of herring ds-DNA, complimentary adsorption of herring ss-DNA on herring ss-DNA and the subsequent formation of a herring DNA multilayer. The same sequence is observed for kinetics of adsorption of salmon DNA in Fig. 3b. The time of adsorption of ss-DNA is in the range of 10-15 min, which is slightly larger than that for adsorption of ds-DNA (7-10 min), which could be due to a larger number of electrically charged sites in the DNA double helix.

*3.3. AFM study.*

A series of typical tapping mode AFM images of adsorbed layers of DNA are shown in Figure S4 (supplementary information). Values of mean surface roughness <rms> evaluated from AFM images are presented in Table 3. The parameter of <rms> is defined as a deviation of the Z values within a defined box calculated as $< rms >= \sqrt{\left(\sum Z_i^2 / m\right)}$, where $Z_i$ is the height value in *i*-point of the image, and *m* is the number of points within the box. It is important to realise that AFM only gives a measurement of surface roughness and not overall film thickness. Silicon substrates were chosen because polished pieces of silicon wafer have a flat surface which is extremely suitable for AFM study whereas evaporated gold films have an inherent roughness. Although the adsorbed molecular layers on gold surface may look slightly different in AFM, the main goal was to investigate relative changes in the film morphology after binding the second layer of ss-DNA and therefore a substrate with minimal roughness was utilised. The observed increase in the film roughness as a result of the second stage of DNA adsorption is the result invariant of the type of the initial surface used.

An adsorbed layer of PEI is rather smooth (AFM image is not shown) with the mean roughness of 0.62 ± 0.03 nm. Adsorption of DNA on top of this film leads to substantial increase in roughness. The adsorbed layer of ds-DNA clearly shows larger grains in Fig. 5a and larger roughness of 1.90 ±0.42 nm, as compared to adsorbed layer of ss-DNA in Fig. S4b having mean roughness of 1.18 ± 0.1 nm. The larger roughness could be due to ds-DNA being much less flexible than ss-DNA, making close chain to chain packing and formation of a smooth film much more difficult. The adsorbed layer of RNA appeared to have completely different morphology (Fig. S4c) with the largest mean roughness of 2.06 ± 0.09 nm, possibly again due to the relative inflexibility of this chain and its tendency to form secondary structures. A second adsorption of complementary ss-DNA (Fig. S4d) on ss-DNA layer adsorbed on PEI gives rise to a film with a slightly larger grain size (perhaps a function of the thicker film) as compared to that obtained from a film exposed to a solution of non-complementary ss-DNA (Fig. S4e); however their values of mean roughness obtained on several samples are very similar.

## 4. Conclusions

The method of electrostatic self-assembly was successfully implemented for adsorption of both single strand and double stranded DNA, as well as RNA. Single stranded DNA electrostatically adsorbed on the solid substrates, (despite the limited degree of freedom), is capable of binding further ss-DNA subsequently forming a DNA multilayer structure with some degree of species selectivity. The results obtained by a sensitive optical technique of total internal reflection ellipsometry proved this concept: the observed changes in thickness due to binding of complementary ss-DNA layers are 5-6 times larger than those observed for non-complementary binding of ss-DNA. Direct AFM observations of the morphology of adsorbed DNA (RNA) layers are in line with TIRE data. The results allow a better understanding of the binding processes that are occurring and combined with our previous electrochemical results show a possibility for the development of rapid and inexpensive electrochemical DNA analyses of natural substances of food, drinks, fabric, wool and other biologically derived materials with sensitivities for genomic DNA in the 0.01 mg $ml^{-1}$ to 1 mg $ml^{-1}$ range and down to 1 fg $ml^{-1}$ for single gene DNA. Future work will involve the optimisation of the conditions of the binding, such as temperature and ionic strength to maximise sensitivity and selectivity of the process.

## Acknowledgement

The authors would like to thank the BBSRC for funding for FD as part of the Centre for Bioarray innovation within the post-genomic consortium. Thanks should also go to Dr Lee Larcombe (Cranfield Health) for gel electrophoresis experiments and helpful discussions.

**References**

Arwin, H., Poksinski, M., Iohansen, K. 2004,Appl. Optics, 43, 3028-3036.

Azzam R.M.A. and Bashara N.M., 1987, Ellipsometry and Polarized Light; North-Holland Personal Library.

Ausubel, F.M., Brent, R., Kingston, R E., Moore, D.D., Sedman, G.G., Smith, J.A., Struhl, K.S., 1993, Current Protocols in Molecular Biology, Vol. 1-2; John Wiley & Sons, New York,.

Bjork, P., Persson, N.K., Peter, K., Nilsson, R., Asberg, P., Inganas, O., 2005, Biosens. Bioelec, 20, 1764-1771.

Britten, R.E., Kohne, D.E., 1968, Science, 161, 529-540.

Cardenas, M., Braem, A., Nylander, T., Lindman, B., 2003, Langmuir, 19, 7712-7718.

Davis, F., Nabok, A.V., Higson, S.P.J., 2005, Biosens. Bioelec, 20, 1531-1538.

Davis, F., Hughes, M A., Cossins, A.R., Higson, S.P.J., 2007, Anal. Chem, 79, 1153-1157.

Delmonte, C.S,.Mann, L.R.B., 2003, Current Science, 85, 1564-1570.

Downs M.E.A., 1991, Biochem. Soc. Trans., 19, 39-43.

Hwang, S., Kim, E., Kwak, J., 2005, Anal. Chem., 77, 579-584.

Korri-Youssufi, H., Garnie, F., Srivastava, P., Godillot, P., Yassar, A., 1997, J. Am. Chem. Soc., 119, 7388-7389.

Kumpubu-Kalemba, L., Leclerc, M. 2000, Chem. Comm., 19, 1847-1848.

Leclerc, M., 1999, Adv. Mater., 11, 1491-1498.

Leff, D.V., Brandt, L., Heath, J.R., 1996, Langmuir, 12, 4723-4730.

Legay, G., Finota, E., Meunier-Prest, R., Cherkaoui-Malki, M., Latruffe, N., Dereux, A., 2005, Biosens. Bioelec, 21, 627-636.

Lemeshko, S.V., Powdrill, T., Belosludsev, Y.Y., Hogan, M., 2001, Nucleic Acids Res., 29, 3051-3058.

Littauer, U.Z.. 2000, Biophysical Chemistry, 86, 259-266.

Lvov, Yu., Decher. G., Sukhorukov. G., 1993, Macromolecules, 26, 5396-5399.

Martin, M.A., Hoyer, B.H., 1966, Biochemistry, 5, 2706-2713.

Mascini, M., Palchetti, H., Marazza,. G. J., 2001, Anal. Chem., 369, 15-21.

McQuade, D.T., Pullen, A.E., Swager, T.M., 2000, Chem. Rev., 100, 2537-2574.

Nabok, A.V., Tsargorodskaya, A., Holloway, A., Starodub, N. F., Gojster, O., 2007, Biosens. Bioelec., 22, 885-890.

Nabok, A.V., Tsargorodskaya, A., Proceedings of 10th European Conference on organised Organic Films, ECOF 10, Latvia, Riga, 24-27 August, 2006, Thin Solid Films, 2007, in press.

Nicollini, C., Erokhin, V., Facci, P., Guerzoni, S., Ross, A., Pashkevich, P., 1997, Biosens. Bioelec,, 12, 613-618.

Park N., Hahn J.H., 2004, Anal. Chem., 76, 900-906.

Poksinski, M., Arwin, H., 2004, Thin Solid Films, 455–456, 716–721.

Rippe, K., Mucke, N., Langowski, J., 1997, Nucleic Acid Research, 25, 1736-1744.

Sato, Y., Kobayashi. Y., Kamiya, T., Watanabe, H., Akaike, T., Yoshikawa,. K., Maruyama, A., 2005, Biomaterials, 26, 703-711.

Steel, A.B., Levicky, R.L., Herne, T.M., Tarlov, M.J., 2000, Biophys. J., 79, 975-981.

Suh, J., Paik, H., Hwang, B.K., 1994, Bioorg Chem 22, 318-327,

Sukhorukov. G., Mohwald, H., Decher, G., Lvov, Y.M., 1996, Thin Solid Films, 284-285, 220-223.

Travas-Sejdic, J., Soman, R., Peng, H., 2005, Thin Solid Films, 497, 96-102.

J.A. Woollam Co., Inc, 2002, Guide to Using WVASE32..

Xi Chun Zhou; Li Qun Huang; Sam Fong Yau Li., 2000, Biosens. Bioelec, 16, 85-95.

## Figure Captions

**Figure 1.** (a) Schematic of TIRE experimental set-up comprising white light sourse (1), polariser (2), analyser (3), photodetector array (4), $68^0$ prism (5), Cr/Au coated glass slide (6), reaction cell (7). (b) typical $\Psi(\lambda)$ and $\Delta(\lambda)$ TIRE spectra of Cr/Au layer deposited on glass. A cross on the $\Delta(\lambda)$ spectrum illustrates the choice of wavelength for kinetics measurements.

**Figure 2.** Series of $\Delta(\lambda)$ spectra taken after following adsorption sequences: (a) (left-to-right) bare Cr/Au film (1), PEI (2), salmon ss-DNA (3), salmon ss-DNA (4); (b) (left-to-right) bare Cr/Au film (1), PEI (2), salmon ss-DNA (3), herring ss-DNA (4).

**Figure 3.** Kinetics of DNA adsorption: (a) herring ss-DNA on PEI (1), salmon ss-DNA on herring ss-DNA (2), herring ds-DNA on PEI (3), herring ss-DNA on herring ss-DNA (4); (b) salmon ss-DNA on PEI (1), herring ss-DNA on salmon ss-DNA (2), salmon ds-DNA on PEI (3), salmon ss-DNA on salmon ss-DNA (4).

**Table 1. Parameters of four-layer model in TIRE fitting** (parameters marked with * were fixed during fitting)

| | |
|---|---|
| ambient: BK7 | $n^*$ = 1.515, $k^*$= 0 at 633 nm |
| 2: Cr/Au | $n^*$ = 0.43±0.11<br>$k^*$ = 3.09±0.19<br>$d^*$= 24.7±2.4 nm<br>at 633 nm |
| 1: Cauchy layer<br>$A_n$*=1.396<br>$B_n$*=0.01<br>$C_n$*=0 | $n^*$= 1.42 , $k^*$ = 0 at 633 nm<br>*d is* a variable parameter (the subject of fitting). The values obtained are given in Table 2 |
| 0: Phosphate buffer solution | $n^*$ = 1.33, $k^*$ = 0 |

**Table 2. Increases in thickness (TIRE data) of different adsorbed layers.**

| **Adsorbed layers** | **Thickness changes* nm (TIRE)** |
|---|---|
| Adsorption initial PEI layer (layer 1) | 2.87 ± 1.24 |
| Adsorption of herring ss-DNA on PEI (layer 2) | 4.22 ± 1.72 |
| Adsorption herring ss-DNA on herring ss-DNA/PEI (layer 3) | 21.81 ± 1.09 |
| Adsorption salmon ss-DNA on herring ss-DNA/PEI (layer 3) | 4.36± 0.36 |
| Adsorption of salmon ss-DNA on PEI (layer 2) | 4.08 ± 1.56 |
| Adsorption salmon ss-DNA on salmon ss-DNA/PEI (layer 3) | 20.47± 0.53 |
| Adsorption herring ss-DNA on salmon ss-DNA/PEI (layer 3) | 3.02± 1.15 |
| Adsorption herring ds-DNA on PEI (layer 2) | 9.75± 1.97 |
| Adsorption salmon ds-DNA on PEI (layer 2) | 8.52± 2.37 |
| Adsorption RNA on PEI (layer 2) | 12.96± 3.14 |

*Thickness changes are additive e.g. Thickness of PEI plus herring ss-DNA layer is 7.09 nm.

**Table 3. Mean roughness (AFM data) of different adsorbed layers.**

| **Adsorbed layers** | **Mean Roughness, nm (AFM)** |
|---|---|
| Adsorption initial PEI layer (layer 1) | 0.62 ± 0.03 |
| Adsorption of herring ss-DNA on PEI (layer 2) | 1.18 ± 0.1 |
| Adsorption herring ss-DNA on herring ss-DNA/PEI (layer 3) | 1.68 ± 0.06 |
| Adsorption salmon ss-DNA on herring ss-DNA/PEI (layer 3) | 1.72± 0.12 |
| Adsorption herring ds-DNA on PEI (layer 2) | 1.90 ±0.42 |
| Adsorption RNA on PEI (layer 2) | 2.06 ± 0.09 |

# The study of genomic DNA adsorption and subsequent interactions using Total Internal Reflection Ellipsometry

**Alexei Nabok[+], Anna Tsargorodskaya[+], Frank Davis[++], Séamus P.J. Higson[++] ***

[+] *Sheffield Hallam University, Materials and Engineering Research Institute, Sheffield, S1 1WB, U.K.*

[++] *Cranfield Health, Cranfield University, Silsoe, MK45 4DT, U.K.*

*Molecular weights of DNA samples.*

The molecular weights of the DNA samples were determined by gel electrophoresis. The salmon DNA consisted mainly of material with a molecular size of 2000bp whereas the herring DNA had a more diverse spread of weight, between 300-1000bp. Samples were run on a 1.2% agarose gel, at 100 V for 30 minutes until the orange loading dye front reached the bottom of the gel to give the widest separation of the samples. The gel was immersed in ethidium bromide to stain the DNA, and visualized using a UV transilluminator and digital camera system (SynGene, UK). The salmon DNA was found (by comparison with a standard DNA ladder) to consist mainly of material with a molecular size of 2000bp whereas the herring DNA had a more diverse spread of weight, between 300-1000bp. Images of the gels can be found below (Figure S1).

*Preparation of substrates.*

Substrates for TIRE measurements were prepared by thermal evaporation of a 3 nm layer of chromium (Cr) onto standard BDH glass slides followed by evaporation of a further 20-25 nm layer of gold (Au) in the same vacuum chamber without breaking the vacuum of $2 \times 10^{-6}$ Pa. Pieces of silicon wafer 10x10 mm in size, cleaned with 5% HF solution and then washed in Millipore water and dried, were used a substrates in AFM experiments.

The following sample preparation procedure and measurements routine were used in this work: An intermediate layer of PEI was deposited onto Cr/Au coated glass slides or pieces of silicon wafers by immersing the substrates into 1 mg/ml solution of PEI for 5 minutes followed by thorough rinsing in Millipore water.

The experimental set-up for TIRE measurements was built on the spectroscopic ellipsometer M2000V (J.A. Woollam Co., Inc.), which is represented on the schematic diagram in Fig. 1a by elements (1-4): the white light source (1), two polarizing prisms (2, 3) called the polarizer and analyzer respectively, and a photodetector array (4). Additional elements, which allow performing TIRE measurements, are a $68^0$ trapezoidal prism (5) with a gold coated glass slide (6) brought into optical contact via index matching fluid, and the reaction cell (7) sealed to the slide through a rubber O-ring. The choice of the prism was dictated by conditions of total internal reflection of light on the glass/water interface. The cell has a volume of 2 ml and contains inlet and outlet tubes to allow injection of different liquids into the cell in order to perform different chemical- and bio-reactions. Elements 5-7 were fixed on the ellipsometer sample stage using vacuum suction.

The spectra of two ellipsometric parameters $\Psi$ and $\Delta$, representing, respectively, the amplitude (A) ratio $\tan(\Psi) = A_p / A_s$ and phase shift $\Delta = \varphi_p - \varphi_s$ between *p*- and *s*- components of polarized light, were recorded using the M2000V instrument in the 350–1000 nm spectral range using the rotating analyzer principle. Optical parameters of the reflection system, i.e. thicknesses and refractive indices of the substrate and adsorbed layers, can be obtained by numerically solving a reverse ellipsometric equation:

$$\tan(\Psi) \cdot \exp(i\Delta) = R_p / R_s .$$

Here $R_p$ and $R_s$ are Fresnel reflection coefficients for p- and s- components of polarized light, respectively, related to the parameters of the reflection system and particularly the thickness (d) and refractive index (n) of the adsorbed layers via Fresnel equations (Azzam *et al* 1987) and $i = \sqrt{-1}$. The fitting is performed by solving Fresnel equations many times for different values of *n* and *d* and subsequently minimizing the error function of experimental and theoretical (calculated) values of $\Psi$ and $\Delta$ using one of least-square techniques. Commercial WVASE32® software is provided by J.A. Woollam Co., Inc. for this task. More details of this technique can be found in our previous papers (Nabok *et al* 2007, Nabok and Tsargorodskaya, 2007).

*Preparation of DNA solutions.*

All water used was purified with a ELGA Purelab UHQ purifier. Phosphate buffer (pH 7) was made by dissolving $NaH_2PO_4H_2O$ (0.55 g), $Na_2HPO_412H_2O$ (2.11 g) and NaCl (7.73 g) in water and making up to 1 litre. DNA of two species of fish, namely herring (Cat. No. D6898) and salmon (Cat. No. D1626), were selected for this study. Both materials were purchased from Sigma Aldrich, as was RNA from *Torola* yeast. DNA solutions, 0.2 mg/ml solutions in phosphate buffer (pH 7) were used in this study.

*Fitting of TIRE data.*

Fitting of the experimental results was performed with WVASE® software using a four layers model, which is shown in Table 1 and described in more detail in previous work (Nabok *et al* 2007, Nabok, A. V., Tsargorodskaya 2007). . Because of the inverted geometry in TIRE measurements, the ambient was the BK7 glass (prism, glass slide) with the optical parameters taken from the WVASE®32 library (Woollam 2002). Layer 2 represents the Cr/Au coating, parameters of which were obtained by fitting the data for uncoated Cr/Au slides. Typical values of d (thickness), n (refractive index), and k (extinction coefficient) for Cr/Au at 633 nm are given in Table 1. Parameters of Layer 2 were kept fixed in subsequent fitting steps. Layer 1 was the organic film represented by Cauchy dispersion formula for refractive index (Woollam 2002):

$$n(\lambda) = A + \frac{B}{\lambda^2} + \frac{C}{\lambda^4},$$

where *A, B* and *C* were parameters of fitting, $\lambda$ is the wavelength of the light and *d* the thickness of the layer.

The extinction coefficient $k = 0$ was used for optically transparent organic layers. In order to simplify fitting, parameters A, B, and C were kept constant during fitting for all organic layers used, so that the value of refractive index was constant (n=1.42) at $\lambda$=633 nm. In this case, the fitting was performed for the thickness *(d)* only. This means that all changes on the gold surface caused by consecutive adsorptions of PEI, ss-DNA and further DNA adsorption are associated solely with the changes in the thickness of the adsorbed layer. Such an approximation is not strictly correct but forms the basis of the most logical model. Finally, Layer 0 (the substrate) was a phosphate buffer aqueous solution approximately described by dispersion data for water (*n*=1.33, k=0 at 633 nm).

*References.*

Azzam R.M.A. and Bashara N.M., 1987, Ellipsometry and Polarized Light; North-Holland Personal Library.

J.A. Woollam Co., Inc, 2002, Guide to Using WVASE32.

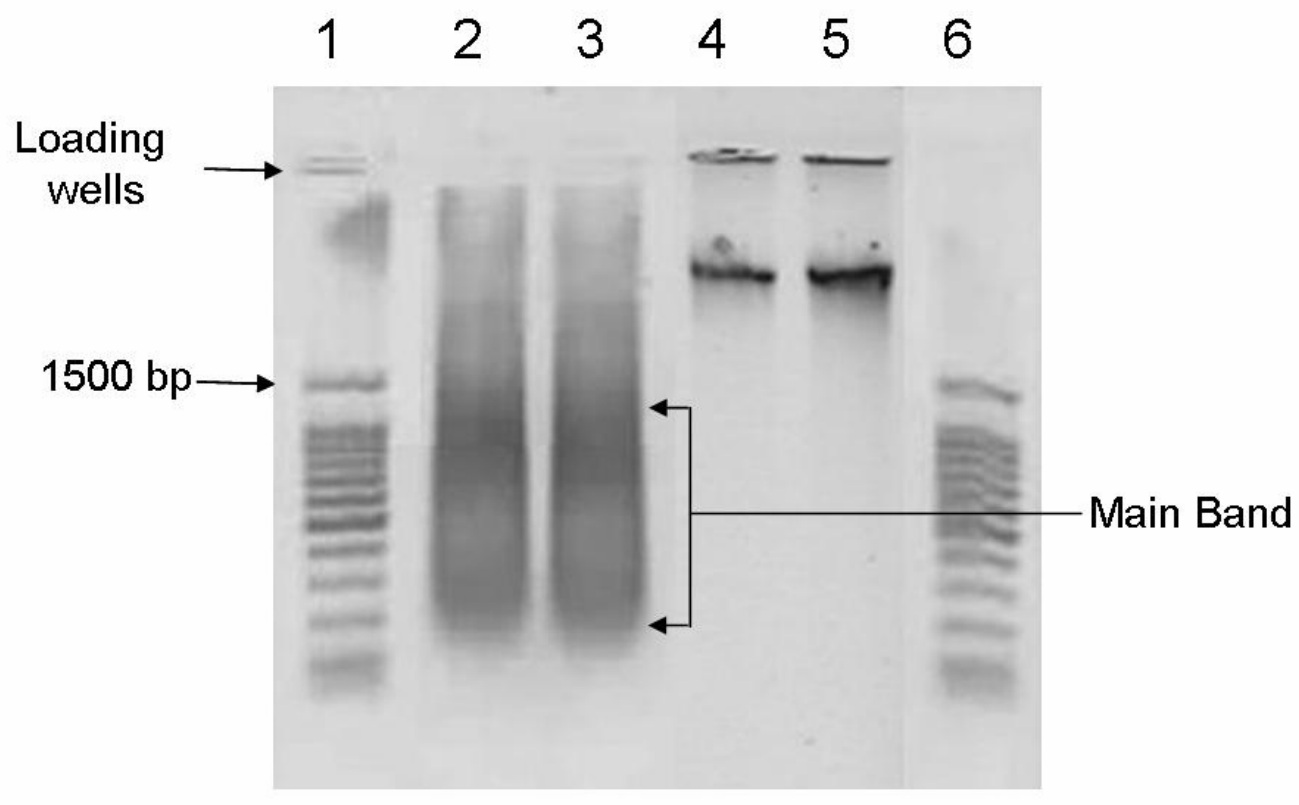


**Figure S1.** The molecular weights of the DNA samples as determined by gel electrophoresis. Size ladder in lane 1 and 6 (1500bp as marked). Herring DNA in Lanes 2 & 3. Salmon DNA in Lanes 4 & 5. Samples were run on a 1.2% agarose gel, at 100 V for 30 minutes and stained with ethidium bromide.

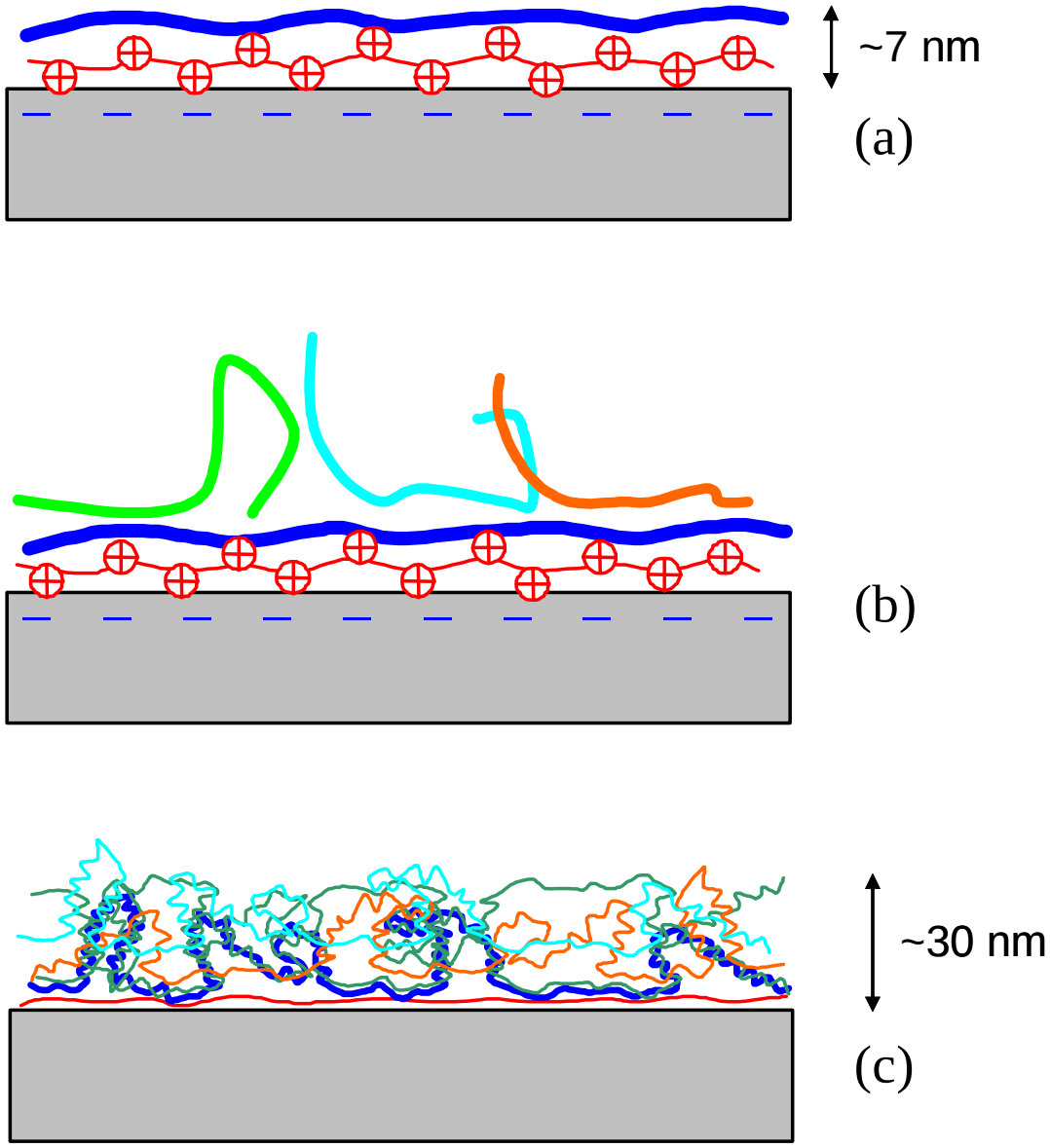


**Figure S2.** Model of adsorbed DNA layers: (a) electrostatic adsorption of first ss-DNA layer onto polycation layer by electrostatic interaction, (b) adsorption of complementary ss-DNA on top of first ss-DNA layer with parts of the strands pendant to the surface, (c) adsorption of further ss-DNA accompanied with crosslinking and tangling which leads to formation of a thick (c 20 nm) DNA layer.

**Figure S3.** AFM tapping mode images of (a) bare Si; (b) Si coated with PEI.

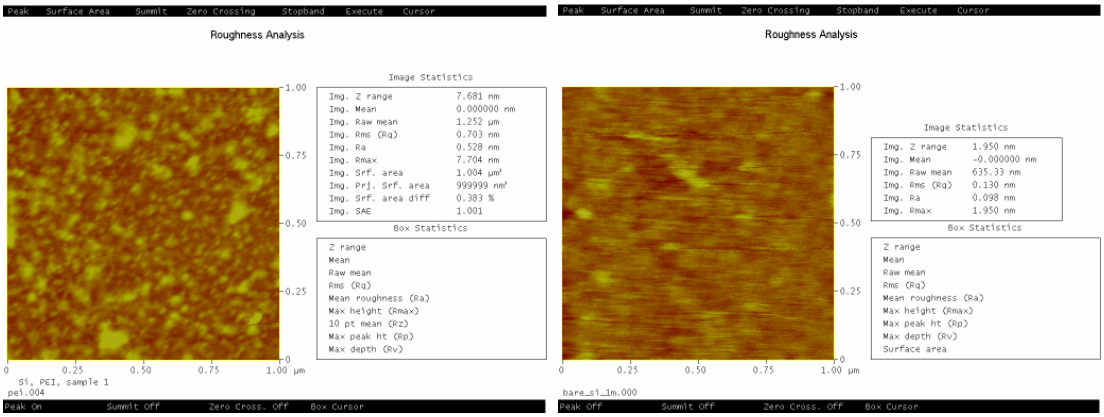


(a) (b)

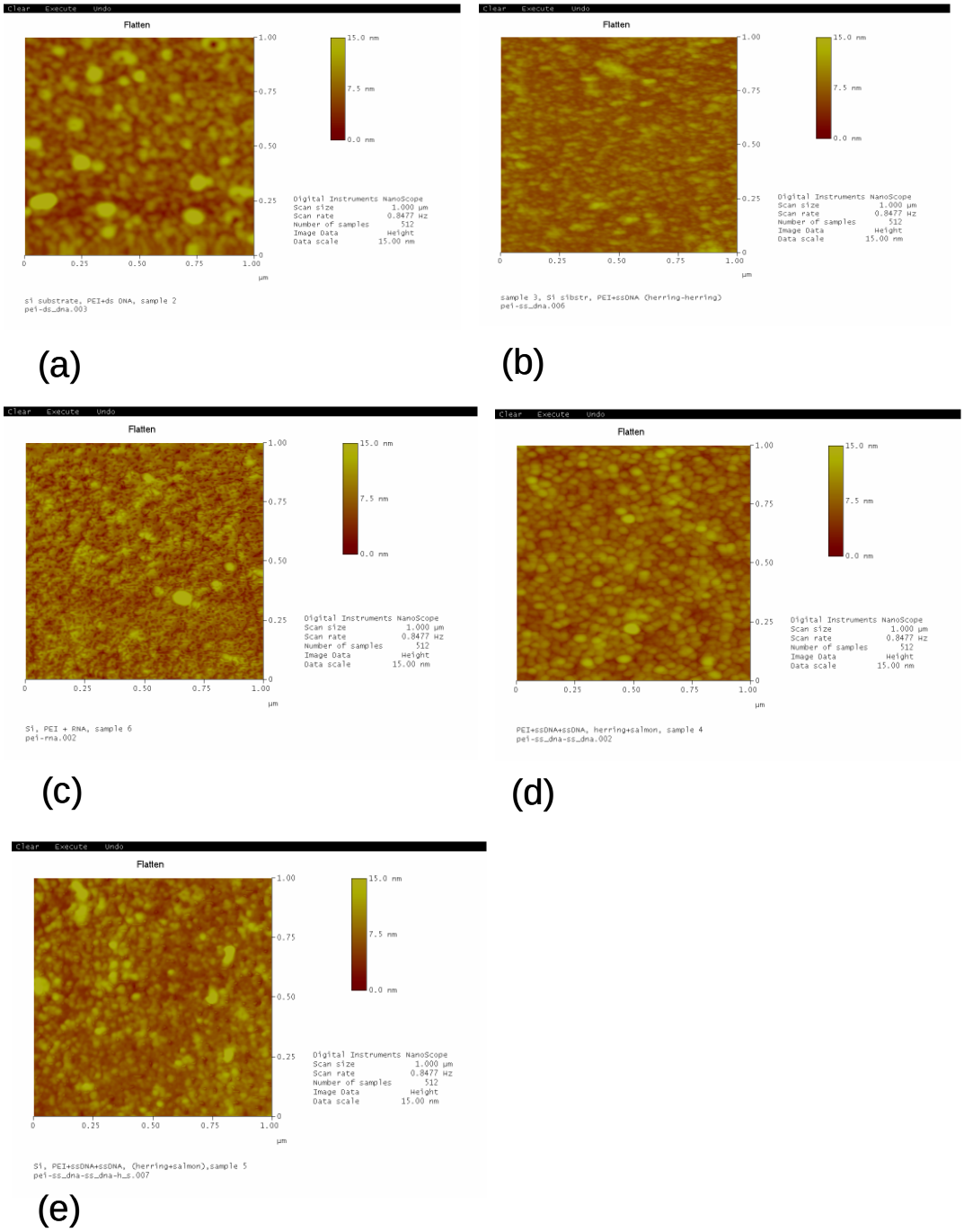


**Figure S4.** AFM tapping mode images of layers of herring ds-DNA (a), herring ss-DNA (b), and RNA (c) electrostatically adsorbed on PEI layer. AFM tapping mode images of layers of herring ss-DNA (d) and salmon ss-DNA (e) adsorbed on top of the layer of herring ss-DNA.